Surface light-induced drift of CH_3F

R. W. M. Hoogeveen, G. J. van der Meer, and L. J. F. Hermans
Huygens Laboratory, Leiden University, P. O. Box 9504, 2300 RA Leiden, The Netherlands
(Received 18 June 1990)

Surface light-induced drift arises under velocity-selective excitation of a low-pressure gas if the accommodation coefficient α for tangential momentum transfer to the surface depends on the state of the gas particles. A kinetic description of this effect is presented. Experiments were performed for rovibrationally excited CH_3F colliding with a quartz surface at 300 K. It is found that α depends on the rotational state (J,K) of the molecule much more strongly than on the vibrational state. For the transition $(J,K)=(4,3)\rightarrow(5,3)$, α is found to increase by $\delta\alpha=1.9\times10^{-3}$. This result is shown to be primarily due to the change in magnitude of the rotational angular momentum $\mathbf{J}$, while its orientation with respect to either the molecular figure axis or the surface normal plays a negligible role.

I. INTRODUCTION

The prediction of light-induced drift (LID) in 1979 by Gel'mukhanov and Shalagin[1] opened up a new field of research. LID arises when gas particles are excited in a velocity-selective way by means of the Doppler effect. Due to a difference in collision properties between excited- and ground-state particles a net drift can occur. In most experiments a (nonabsorbing) buffer gas is used as a collision partner;[2] in that case, the drift occurs due to a state-dependent collision cross section of the absorbing species with respect to the buffer gas. These experiments can provide information about excited-state potentials (see Ref. 3). However, it is also possible to perform LID experiments in a pure gas, where the wall takes over the role of the buffer gas. In this case a difference in molecule-surface interaction between excited- and ground-state particles gives rise to a drift of the gas. This phenomenon, surface light-induced drift (SLID), was predicted in 1983 by Ghiner *et al.*[4] and experimentally demonstrated in 1987.[5]

The basic idea of SLID is illustrated in Fig. 1. A single mode laser beam shines through a capillary cell (in the positive x direction). The cell contains an optically absorbing gas at such low pressure that molecule-wall collisions dominate (Knudsen regime). If the frequency of the laser, ω_L, is slightly detuned from the center of the absorption line at ω_0, only those molecules are excited which compensate the detuning with their Doppler shift. As a result, excited molecules will have an x velocity in a narrow band around $v_L=(\omega_L-\omega_0)/k$, where k is the magnitude of the wave vector. If the accommodation coefficient for parallel momentum transfer, α, differs for excited- and ground-state particles a net momentum transfer to the wall occurs. In an open tube this will result in a drift of the total gas in the direction of the particles having the smaller accommodation. In a closed tube a pressure gradient will build up.

In the next section, theoretical expressions will be derived for the drift velocity in an open tube and for the pressure difference in case of a closed tube. In Sec. III the setup and the experimental procedure are outlined. Experiments on SLID of CH_3F, rovibrationally excited by a tunable CO_2 laser, in a quartz capillary at 300 K will be discussed in Sec. IV.

II. THEORY

The theoretical treatment of the SLID phenomenon given here will be analogous to that of LID as given in Ref. 6. A two-level model will be assumed (see Fig. 2) where the excited-state velocity distribution will be denoted by $f_e(\mathbf{v})$ and the ground-state distribution by $f_g(\mathbf{v})$. Integration over the velocities yields the corresponding densities, $n_{\rm exc}=\int f_e(\mathbf{v})d\mathbf{v}$ and similarly for n_g, such that $n=n_{\rm exc}+n_g$ is the total number density. (Later, a second excited-state density will be introduced. This new quantity, n_e, will have the meaning of the density of molecules that have just been excited but have not yet suffered a velocity-randomizing collision. It is therefore smaller than $n_{\rm exc}$ which also contains molecules from the excited-state Maxwellian.) The laser which populates the excited state is assumed to be not perfectly velocity selective in order to allow for a nonzero homogeneous line broadening. Within the two levels, velocity-randomizing collisions take place at a rate ν_g for ground-state particles and ν_e for excited particles. It is assumed that in the excited state a fraction γ of these collisions also changes the vibrational state of the molecule.

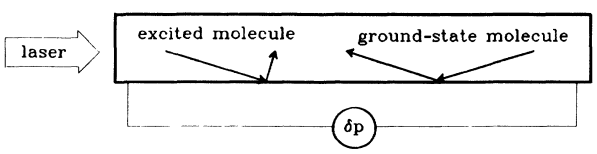

FIG. 1. Principle of surface light-induced drift. Under velocity-selective excitation, parallel momentum is transferred to the surface if the accommodation is state dependent. This will give rise to a drift of the (Knudsen) gas in an open cell, or to a pressure difference in a closed cell.

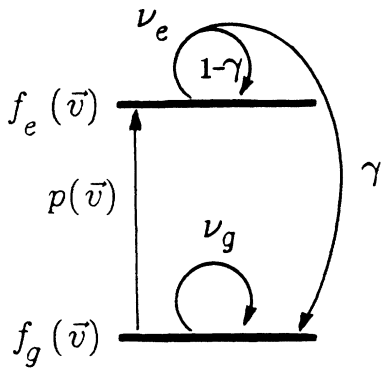

FIG. 2. Scheme of the levels and rates relevant for SLID.

Radiative decay is not included in the model since the lifetime for this process is too long (on the order of 1 s, see Ref. 7). Furthermore, the light distribution in the cell will be assumed uniform (small absorption over the length of the cell). This means that in an open cell no gradients will occur.

The stationary-state distributions for the excited and ground states, $f_e(\mathbf{v})$ and $f_g(\mathbf{v})$, respectively, can be obtained from the following rate equations:

$$np(\mathbf{v})-\nu_e f_e(\mathbf{v})+\nu_e(1-\gamma)n_{\text{exc}}W(\mathbf{v})=0\ , \tag{1}$$

$$-np(\mathbf{v})-\nu_g f_g(\mathbf{v})+(\nu_g n_g+\nu_e\gamma n_{\text{exc}})W(\mathbf{v})=0\ . \tag{2}$$

Here, $p(\mathbf{v})d\mathbf{v}$ is the contribution to the excitation rate from the velocity interval between $\mathbf{v}$ and $\mathbf{v}+d\mathbf{v}$. [It is chosen here to define the pump term as $np(\mathbf{v})$ rather than $n_g p(\mathbf{v})$ since this will turn out to be more convenient in later equations.] In Eqs. (1) and (2), $W(\mathbf{v})$ is the normalized Maxwell distribution

$$W(\mathbf{v})=(m/2\pi k_B T)^{3/2}\exp\left[\frac{-mv^2}{2k_B T}\right]\ , \tag{3}$$

with m the mass of the particle, k_B Boltzmann constant, and T the temperature.

Integration of Eq. (1) over velocities yields n_{exc}:

$$n_{\text{exc}}=\frac{nP}{\nu_e\gamma}\ , \tag{4}$$

where $P=\int d\mathbf{v}\,p(\mathbf{v})$ is the excitation rate. Expressions for $f_e(\mathbf{v})$ and $f_g(\mathbf{v})$ can be derived if Eq. (4) is substituted in Eqs. (1) and (2):

$$f_e(\mathbf{v})=\frac{(1-\gamma)nPW(\mathbf{v})}{\nu_e\gamma}+\frac{np(\mathbf{v})}{\nu_e}\ , \tag{5}$$

$$f_g(\mathbf{v})=\left[n_g+\frac{nP}{\nu_g}\right]W(\mathbf{v})-\frac{np(\mathbf{v})}{\nu_g}\ . \tag{6}$$

It is seen that both distributions consist of a Maxwellian with a peak in the excited state and a dip in the ground state at the resonant velocity.

Since the total distribution $f(\mathbf{v})=f_g(\mathbf{v})+f_e(\mathbf{v})$ is known, the drift velocity can be calculated:

$$\mathbf{v}_d=\frac{1}{n}\int d\mathbf{v}\,\mathbf{v}f(\mathbf{v})$$

$$=\left[\frac{1}{\nu_e}-\frac{1}{\nu_g}\right]\int d\mathbf{v}\,\mathbf{v}p(\mathbf{v}) \tag{7}$$

[the terms containing $W(\mathbf{v})$ vanish since they are odd in $\mathbf{v}$].

We assume small absorption such that for the excitation probability a Voigt function can be taken:

$$p(\mathbf{v})\propto\frac{W(\mathbf{v})}{\Gamma_B^2+(\Omega-\mathbf{k}\cdot\mathbf{v})^2}\ . \tag{8}$$

Here, Γ_B is the homogeneous linewidth of the transition and Ω the detuning from line center, $\Omega=\omega_L-\omega_0$. Mironenko and Shalagin[8] have shown that it is convenient to define

$$\varphi(\Omega)=\frac{\int d\mathbf{v}\,\mathbf{k}\cdot\mathbf{v}p(\mathbf{v})}{kv_0P}\ , \tag{9}$$

where $v_0=\sqrt{2k_BT/m}$. A graph of $\varphi(\Omega)$ for various homogeneous linewidths is given in Fig. 3. Substitution of Eq. (9) in Eq. (7) results in

$$\mathbf{v}_d=\left[\frac{1}{\nu_e}-\frac{1}{\nu_g}\right]Pv_0\varphi(\Omega)\frac{\mathbf{k}}{k}\ . \tag{10}$$

In order to relate ν_e and ν_g to the accommodation coefficient for parallel momentum transfer, we observe that in the low-pressure regime (Knudsen limit) the velocity-randomizing collisions take place only at the cell wall. The rate for molecule-wall collisions is $\bar{v}/2R$ where $\bar{v}=\sqrt{8k_BT/\pi m}$ is the mean thermal speed (since the number of molecule-wall collisions per second is $\frac{1}{4}n\bar{v}2\pi RL$ and the number of molecules in the volume is πR^2Ln). However, in molecule-wall collisions, on the average only a fraction α of the initial tangential momentum of the particle is transferred to the wall. The frac-

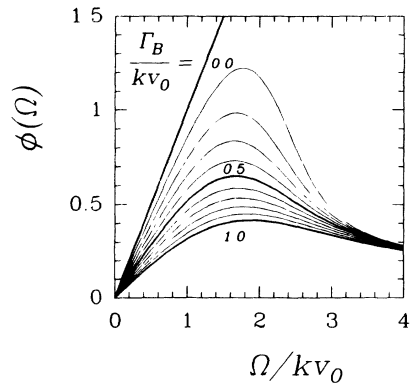

FIG. 3. Detuning function $\varphi(\Omega)$ for different homogeneous linewidths. For δ-peak excitation ($\Gamma_B=0$), $\varphi(\Omega)$ can be approximated by $\Omega/kv_0=v_L/v_0$.

tion α is by definition the accommodation coefficient for parallel momentum transfer. In Maxwell's model for molecule-wall collisions, with only purely specular and purely diffusive collisions possible, the coefficient α is the probability that a particle scatters diffusively (and thus transfers all of its parallel momentum to the wall). If α is not unity, the above collision rate is to be reduced by α in order to find the rate of velocity-randomizing collisions. Thus a state-dependent accommodation gives rise to the state-dependent effective collision rate:

$$\nu_{e,g}=\alpha_{e,g}\frac{\bar{v}}{2R} . \tag{11}$$

If n_e is now introduced as the density of excited particles which are still in the proper velocity interval around v_L, the excitation rate P in Eq. (10) can be substituted according to

$$n_e=\frac{nP}{\nu_e}=\frac{nP}{\alpha_e(\bar{v}/2R)} . \tag{12}$$

Note that nP can be easily related to the absorbed laser intensity ΔI in the actual experiment by $nP=\Delta I/\hbar\omega_L L$ where $\hbar\omega_L$ is the photon energy and L the cell length.

Using Eqs. (11) and (12), Eq. (10) can be written as

$$\mathbf{v}_d=-\left[\frac{\alpha_e-\alpha_g}{\alpha_g}\right]\frac{n_e}{n}v_0\varphi(\Omega)\frac{\mathbf{k}}{k} , \tag{13}$$

where $\varphi(\Omega)$ reduces to v_L/v_0 for infinitely small homogeneous linewidth ($\Gamma_B \ll kv_0$, i.e., δ-peak excitation) and not too large detuning. The resulting expression for v_d is identical to that for LID in a buffer gas (see Ref. 2) if α is replaced by σ, the kinetic cross section of the particle.

In a closed tube, the drift of the gas will build up a pressure difference, $\delta p \equiv p_{\text{exit}}-p_{\text{entrance}}$, between the ends of the cell. To obtain an expression for δp one has to balance the light-induced flux with the free molecular (Knudsen) back flow:[9]

$$\pi R^2 v_d=\frac{4\sqrt{\pi}}{3}\frac{R^3 v_0}{p}\frac{2-\alpha}{\alpha}\frac{\delta p}{L} , \tag{14}$$

where α is the value of the tangential accommodation coefficient averaged over all particles. Substitution of Eq. (13) in (14) results in an expression for the relative pressure difference:

$$\frac{\delta p}{p}=-\frac{3\sqrt{\pi}}{4}\frac{L}{R}\left[\frac{\alpha_e-\alpha_g}{\alpha_g}\right]\frac{\alpha}{2-\alpha}\frac{n_e}{n}\varphi(\Omega) . \tag{15}$$

Equation (15) can be simplified by making the approximations $\alpha_g \approx \alpha \approx 1$ (justified in the present experiment) and $\varphi(\Omega)\approx v_L/v_0=(4/\pi)^{1/2}v_L/\bar{v}$ (for δ-peak excitation) resulting in

$$\frac{\delta p}{p}=-\frac{3}{2}\frac{L}{R}\frac{n_e}{n}\frac{v_L}{\bar{v}}(\alpha_e-\alpha_g) . \tag{16}$$

This is essentially identical to the result of the elementary model of Ref. 5 apart from a factor $3\pi/8$.

III. EXPERIMENTS

The experiments were performed with the symmetric top molecule CH_3F, either with the natural mixture (98.9 wt. % ^{12}C) or with the ^{13}C isotopic species (99 wt. % ^{13}C). The molecule has an absorption band around 10 μm which is due to rovibrational excitation of the ν_3 mode, i.e., C—F stretch. Coincidences between CH_3F absorption lines ($v=0\rightarrow 1$) and CO_2-laser lines were calculated using the CH_3F data of Refs. 10 and 11 for ^{12}C and ^{13}C, respectively, and the CO_2 data of Ref. 12. These calculated coincidences were found to be accurate within a few MHz, even for the high J values. The CO_2 laser was equipped with a grating for line selection. The output mirror was mounted on a piezoelectric element for fine tuning. The tuning range was 260 MHz being the free spectral range of the waveguide laser. If necessary the effective tuning range was extended by using an extra cavity acousto-optic modulator (IntrAction model AGM-903), shifting the frequency by 90 MHz either way, or 180 MHz either way when used in the double pass configuration. Thus a total tuning range of 620 MHz was achieved.

The cell consists of a temperature controlled quartz capillary (diameter 1.5 mm, length 300 mm, unless stated otherwise) suspended between two stainless steel mounts on which barium fluoride Brewster windows and the vacuum connections are mounted (see Fig. 4). A thermocou-

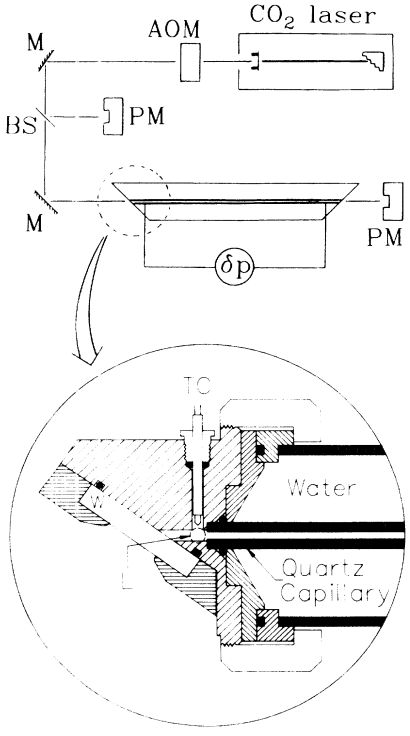

FIG. 4. Scheme of the experimental setup (AOM, acousto-optic modulator for frequency shifting; M, mirror; BS, beam splitter; PM = power meter; TC = thermocouple; W = window; L = lead to differential manometer, perpendicular to the plane of drawing).

ple, in direct contact with the gas, monitors the difference in gas temperature between entrance and exit of the cell. This signal is used to provide information on possible temperature-induced spurious effects (see Sec. V). The pressure difference between the ends of the capillary was measured by a differential capacitance manometer (Datametrics 570 D) with a sensitivity of 10^{-4} Pa. The same manometer was also used to measure the absolute pressure in each experiment. Two thermopile power meters were used to register the absorption of light; one monitors a fraction of the ingoing laser power, the other the transmitted power. The loss of light in the vacuum cell was low, ~20%, and is primarily due to incoupling losses at the entrance of the cell. The sensitivity of the power meters was adjusted in such a way that the difference between the signals gives zero in the vacuum cell. With this differential technique, the absorbed laser power, ΔP_L, was measured with a sensitivity of 1 mW at a typical laser power of 1 W. From the absorption, the density of excited particles that are still in the proper velocity interval, n_e, can be calculated according to Eq. (12) in the Knudsen limit. However, since most experiments were performed in the pressure interval where intermolecular collisions cannot be neglected, the collision rate ν_e in Eq. (12) consists not only of molecule-wall collisions at a rate $\alpha_e \bar{v}/2R$ but also of intermolecular collisions at the kinetic rate ν_k, leading to

$$n_e = \frac{\delta P_L}{\hbar\omega_L \pi R^2 L}\left(\frac{\alpha_e \bar{v}}{2R}+\nu_k\right)^{-1}. \tag{17}$$

The intermolecular collision rate was calculated from the viscosity according to $\eta = 5nk_BT/4\nu_k$. With $\eta = 11.5 \times 10^{-6}$ Pa s,[13] one obtains $\nu_k = 1.45\times10^7$ s^{-1} at $p = 133$ Pa and $T = 295$ K.

An experiment consists of slowly scanning the laser through the CH_3F absorption profile. Since the pressure response time of the system is short (~10 s in the Knudsen limit down to ~1 s at 133 Pa) the laser power, the absorption, the temperature difference, and the pressure difference can be recorded simultaneously in real time as a function of detuning. A correction on δp may be included to account for the noninfinitely slow scanning through the Doppler profile. In analogy with the RC low-pass filter in electronics, a correction factor of the form $(1+\omega^2R^2C^2)$ was tentatively used to describe the dependence of the measured δp amplitude upon the scanning time ($\propto \omega^{-1}$). To this end, the pressure response time RC was determined in a separate pressure relaxation experiment, and ω was derived using the sinusoidal character of the pressure signal. This procedure was found to given an excellent description of the data. However, all data presented here were obtained for such long scanning times that the correction was always $\lesssim 10\%$ and therefore neglected.

The value of RC used above was also employed to determine the value of α for this system in the absence of laser light. It was found that $\alpha = 0.95\pm0.05$, in agreement with the near-unity value to be expected for such systems.

IV. RESULTS

A. Characteristics of SLID: The $R(4,3)$ data in the Knudsen limit

In this subsection the dependence of SLID on detuning, pressure, and geometry as given by Eq. (15) will be experimentally investigated. To this end, the $R(4,3)$ transition[14] of $^{13}CH_3F$ was used, which is in near coincidence with the $9P(32)$ line of the CO_2 laser (mismatch $\nu_{CH_3F} - \nu_{CO_2} = -26$ MHz).

Figure 5 shows the results of five typical scans, which were taken in a room temperature quartz cell at pressures of 1.5, 2.9, 4.2, 5.5, and 7.0 Pa and at a laser power of 1.3 W, viz., the absorbed power (a) and the pressure difference (b). From the measured absorption profile the homogeneous linewidth, Γ_B, can be deduced to be 13 MHz for all five pressures, resulting in $\Gamma_B/kv_0 = 0.35$. The pressure independence of this value can be understood, since it is largely due to power broadening (the pressure broadening coefficient is 18.3 MHz/133 Pa,[6] resulting in less than 1 MHz pressure broadening for the measurements shown in Fig. 5). In accordance with Eq.

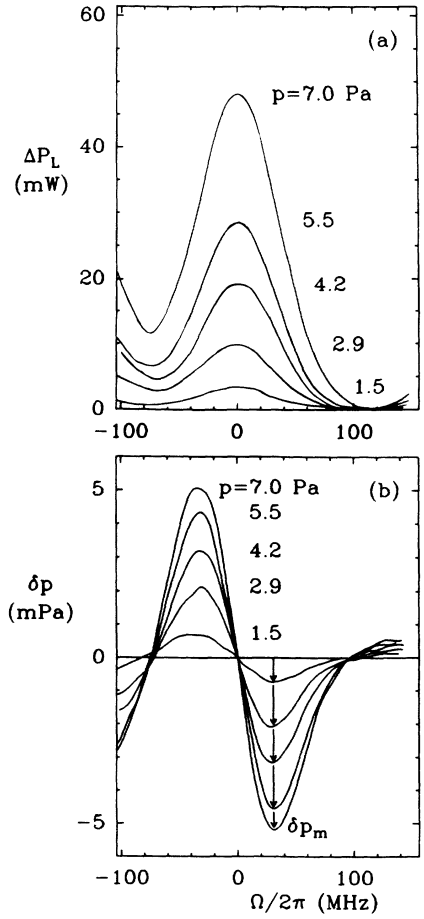

FIG. 5. Typical scans at five different pressures, corresponding to $\bar{l}/R = 0.74$ up to 3.5; (a) measured absorbed power in mW; (b) observed pressure difference over the tube. The scanning time was 4.5 minutes.

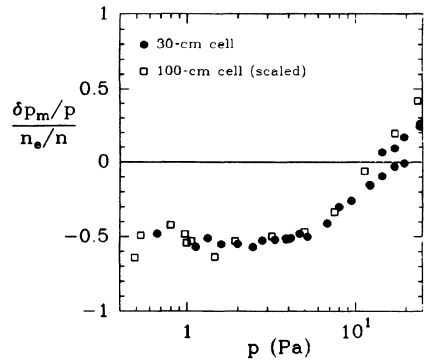

FIG. 6. Values of $(\delta p_m/p)(n_e/n)^{-1}$ for the $R(4,3)$ transition as a function of pressure, taken at 295 K in a quartz cell. The circles are taken in a cell with length 30 cm, the squares in a cell of 100 cm (reduced by a factor of 3.3 for easy comparison). The value $\bar{l}/R=1$ is reached at $p=5.1$ Pa.

(15), δp is seen to be odd in detuning. The asymmetry is caused by the neighboring absorption lines $R(4,2)$ (mismatch -158 MHz) and $R(4,4)$ (mismatch $+165$ MHz). Note that δp is two orders of magnitude larger than what is expected from radiation pressure ($\delta p_{\rm rad}=\Delta I/c$, with c the speed of light).

The maximum value of the pressure effect at positive detuning, δp_m, normalized by the pressure and the excited-state fraction n_e/n at that detuning, is plotted as a function of pressure in Fig. 6. It is seen that $(\delta p_m/p)(n_e/n)^{-1}$ tends to a constant value in the low-pressure limit. From this limiting value the difference in accommodation coefficient $\alpha_e-\alpha_g\equiv\delta\alpha$ is calculated using Eq. (15). The value of $\varphi(\Omega)$ used is 0.49; this follows from Fig. 3 for a broadening of $\Gamma_B/kv_0=0.35$ if Ω/kv_0 is given the value corresponding to the detuning for which δp_m is reached [$\Omega/2\pi=30$ MHz which corresponds to $\Omega/kv_0=0.77$, cf. Fig. 5(b)]. It is thus found that the accommodation coefficient for tangential momentum transfer to a quartz surface for a CH_3F molecule in the state $v=1$, $J=5$, $K=3$ is larger than in the state $v=0$, $J=4$, $K=3$ by

$$\frac{\alpha_e-\alpha_g}{\alpha_g}\frac{\alpha}{2-\alpha}\approx\alpha_e-\alpha_g=(1.9\pm0.3)\times10^{-3}\ ,$$

where the approximation $\alpha_g\approx\alpha\approx1$ was used.[15]

The dependence of SLID on geometry was tested in experiments with a tube of the same diameter but with a length of 100 cm. According to Eq. (15), this should lead to an increase of the $(\delta p_m/p)(n_e/n)^{-1}$ values by a factor of 3.3 compared to the results obtained in the 30-cm cell. This is indeed found to be the case as seen from the excellent agreement shown in Fig. 6, where the squares show the experimental data for the longer cell, normalized by the factor 3.3. Despite this increase in sensitivity, however, since the response time and noise of the signals increased roughly by the same factor, all other experiments were performed with the 30-cm cell.

B. The $R(4,3)$ data at higher pressures

Outside the Knudsen regime one expects the SLID $(\delta p_m/p)(n_e/n)^{-1}$ value to decrease due to the fact that the molecular back flow of Eq. (14) is assisted by the Poiseuille flow. However, the data in Fig. 6 decrease more rapidly with increasing pressure than expected; the effect even changes sign around 17 Pa (ratio of mean free path to tube radius $=\bar{l}/R\approx0.3$). This is caused by "light-induced viscous flow" (LIVF). This effect arises in case of nonhomogeneous illumination of the tube in combination with a state-dependent collision cross section (see Ref. 16). At the pressure where both effects are of the same magnitude but have different signs, one may at first sight expect the pressure difference to vanish over the entire range of detuning, since both effects have the same detuning behavior. In the experiment, however, the pressure difference as a function of detuning becomes complicated [see Fig. 7(a)]. The inner two extrema have the sign of SLID, the outer two that of LIVF. An explanation for this awkward behavior may be found in the difference in broadening between the two effects. In this pressure interval SLID occurs only near the cell wall (in a layer having a thickness of approximately one mean free path) where the laser intensity and thus the broadening is relatively small. LIVF, however, originates also in brighter parts of the cell, where the broadening is larger. Consequently, also the corresponding pressure effects will exhibit larger broadening [see Fig. 1(b) of Ref. 17]. As a result, even when the amplitudes of the effects are equal, the two do not add up to give zero over the complete frequency interval. To verify this conjecture, computer simulations were made for superpositions of two-light-induced drift signals with different broadening coefficients [Fig. 7(b)]. In these simulations, the broadening for the SLID signal is assumed to be determined by pressure only whereas for the LIVF signal also power broadening was taken into account (set at 10 MHz). The relative weight of the two signals was used as a free parameter to fit the experimental data. Apart from the far wings, which are obscured by the neighboring lines, the agreement with the experimental observations is remarkable.

C. Different rotational sublevels

With excitation of the $R(4,3)$ transition both the vibrational state and the rotational state of the molecule are changed. To separate the influence of these two upon the change in accommodation coefficient, several other rotational sublevels within the ν_3 vibrational transition of the CH_3F molecule were investigated. In Fig. 8, such experimental data are shown in addition to the $R(4,3)$ data over a wider pressure interval. The squares show values of $(\delta p_m/p)(n_e/n)^{-1}$ for the $Q(12,2)$ and $Q(12,3)$ transitions in the $^{12}CH_3F$ species [mismatch resp. $+40$ and $+207$ MHz from the $9P(20)$ CO_2-laser line]. For these Q transitions the low-pressure limit gives a very small value which corresponds to an upper limit of $|\delta\alpha|\leq0.1\times10^{-3}$. (The effect at higher pressure originates from LIVF.[16]) Since in Q transitions the rotational state of the molecule is not changed upon excitation, one is led to conclude

that α depends much more strongly on the rotational state than on the vibrational state.

Some other absorption lines were also tested, namely the $P(24,13)$ line of $^{13}CH_3F$ [mismatch +52 MHz from $10R(30)$], the $Q(18,15)$ of $^{12}CH_3F$ [+164 MHz from $9P(22)$], and the $R(31,9)$ of $^{13}CH_3F$ [−121 MHz from $9R(6)$]. These absorption lines are rather weak so that experiments could only be performed at relatively high pressures. As a consequence, these data do not permit a reliable extrapolation into the low-pressure limit, so that no value for $\delta\alpha$ can be derived for these transitions. The behavior at high pressures is primarily due to the influence of inelastic collisions, as will be discussed in a forthcoming paper.[18] The behavior at low pressure is discussed in Ref. 20.

D. The role of K/J

In order to assess the role in the molecule-surface collision dynamics of the orientation of the rotational axis relative to the figure axis, a complete survey was made over all five $R(4,K)$ lines with $K=0$ through 4. These lines all lie within 600 MHz around the $9P(32)$ laser line. By using the acousto-optic modulator in the double pass configuration (shifting the laser frequency 180 MHz either way) in addition to the unshifted laser line, the complete profile could be taken in three runs. Figures 9(a) and 9(c) give the calculated and the observed absorption, respectively, as a function of frequency at a pressure of 6.7 Pa (the homogeneous linewidth found in this experiment is somewhat smaller, $\Gamma_B/kv_0=0.2$, due to lower

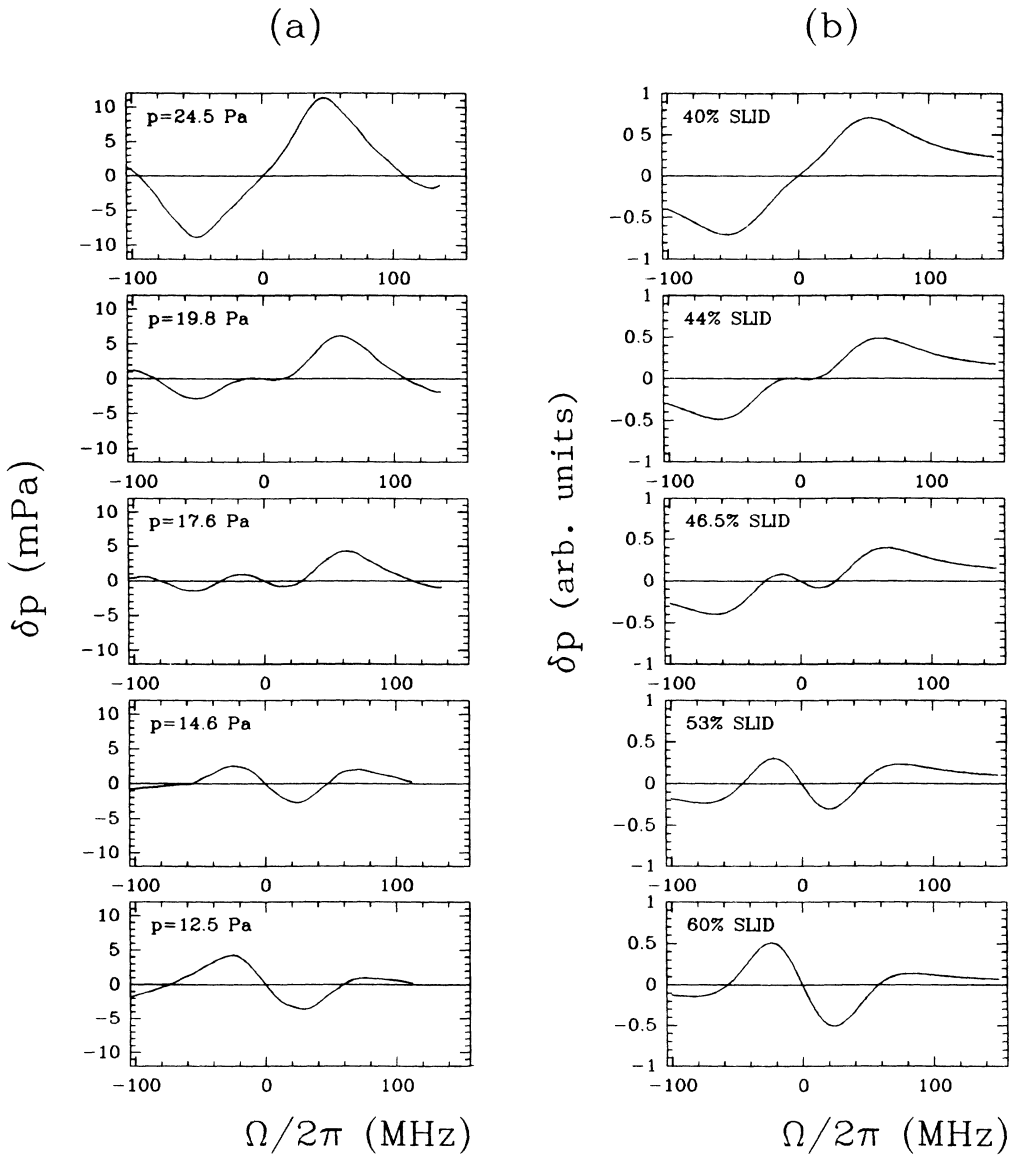

FIG. 7. The pressure difference as a function of detuning for the $R(4,3)$ transition around $\bar{l}/R \approx 0.3$, illustrating the competition between surface light-induced drift and light-induced viscous flow: (a) experimental scans for different pressures; (b) computer simulations for the same pressures (see text).

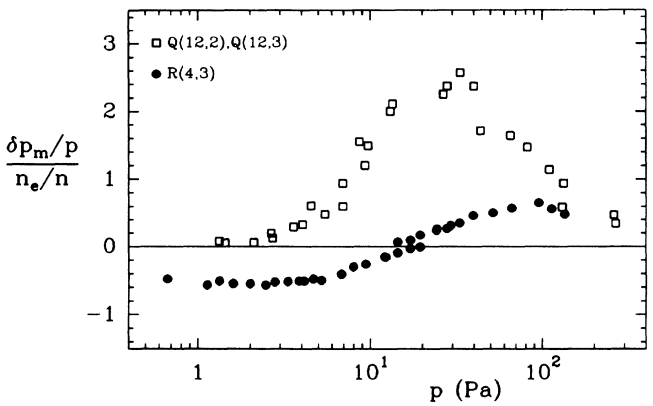

FIG. 8. Values of $(\delta p_m/p)(n_e/n)^{-1}$ as a function of pressure for the transitions $Q(12,2)$ and $Q(12,3)$. The $R(4.3)$ results of Fig. 6 are given for comparison. Note the differences in scales.

laser power used here, $P_L \approx 0.5$ W). Figure 9(d) shows the observed pressure difference whereas Fig. 9(b) shows the pressure difference one would expect if $\delta\alpha$ is independent of the K level involved. The latter is in fact the derivative of the absorption profile as pointed out by Bakarev and Folin.[19] Experiment and calculation are in good agreement, which means that the dependence of α on K (or on K/J) is too weak to be detected in this experiment.

E. The role of the alignment of J

If the gas is irradiated with linearly polarized light (as is done in the above experiments), the excited state will have an anisotropic **J** distribution in the case of a $\Delta J \neq 0$ transition (P and R lines). With vertically polarized light, the molecules in the excited state of the $R(4,3)$ transition will have $J=5$ with their **J** predominantly in the horizontal plane. For circularly polarized light, the molecules in the excited state will have their $J=5$ predominantly parallel or antiparallel with **k**. In either case, an alignment of the angular momenta is produced. Note that any scrambling of this alignment by the earth magnetic field during the free flight can be neglected for nonparamagnetic molecules like CH_3F.

Experiments performed with vertically and circularly polarized light exhibit no difference within the measuring accuracy [Fig. 10(a)], which suggests a negligibly small role of the alignment of **J**. This is confirmed in a more direct experiment in which the circular tube was replaced by a flat channel (cross section 1.0×4.2 mm^2, length 28 cm) made of borosilicate glass. Figure 10(b) shows the result of such experiments performed with the light polarization parallel and perpendicular to the broad side of the channel (it was verified that this polarization was preserved in the transmitted light). Again, the two data sets agree within experimental errors [see Fig. 10(b)], which corroborates the above conclusion. It should be stressed that this does not exclude the existence of align-

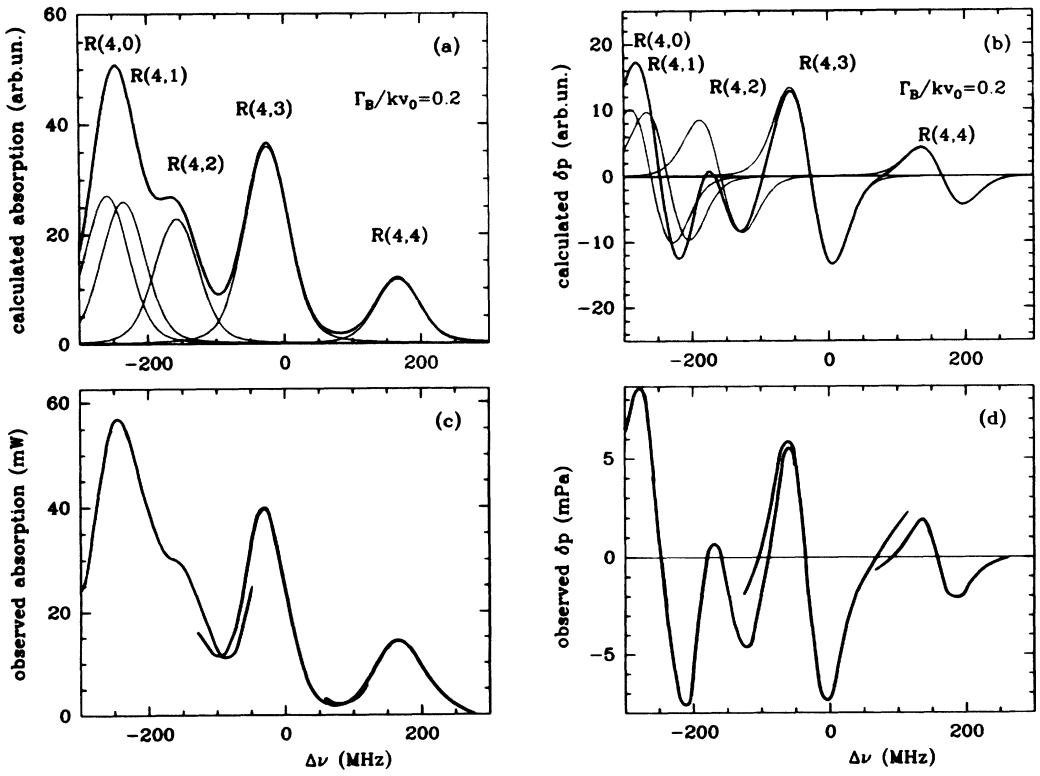

FIG. 9. Calculations (a), (b) and measurements (c), (d) for the $R(4,K)$ transitions; (a) and (c) show the absorbed laser power, (b) and (d) the pressure difference. Frequencies are with respect to the $9P(32)$ laser line center. The experimental curves are composed of three separate scans with different frequency shifts by the AOM.

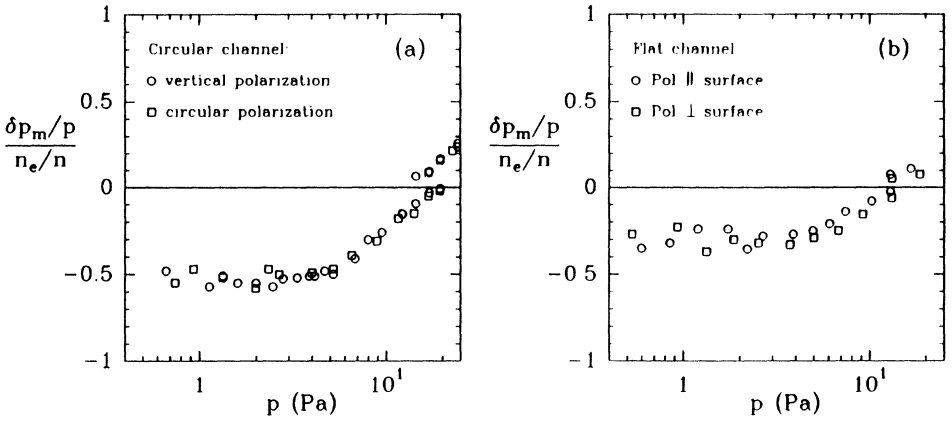

FIG. 10. Values of $(\delta p_m/p)(n_e/n)^{-1}$ for the $R(4,3)$ transition for various light polarizations: (a) linearly and circularly polarized light in a circular tube; (b) horizontally and vertically polarized light in a flat (borosilicate) channel.

ment effects in general. It only indicates that such effects cannot be the prime mechanism behind the results presented here. For a more detailed discussion the reader is referred to Ref. 20.

V. DISCUSSION

From the observations described in Sec. IV C it must be concluded that the accommodation coefficient for tangential-momentum transfer, α, is much more strongly affected by the rotational excitation than by excitation of the ν_3-vibrational mode.

As a possible mechanism to explain the observations, Chapovsky[21] suggested the interaction of the molecule's dipole with its image dipole in the solid. The interaction energy was written as

$$\Delta E \propto \frac{M^2K^2}{J^2(J+1)^2} . \tag{18}$$

Here, M is the projection of J on a fixed axis, e.g., the surface normal. The factor $K^2/J(J+1)$ originates from the projection of the molecule's dipole on the rotational axis, i.e., the part of the dipole which does not rotate around J. From Eq. (18) it can be seen that an anisotropic J distribution (due to excitation of a P or R line, see Sec. IV E) can give an energy change in the molecule-surface interaction, whereas excitation of a Q line does not.

The mechanism of dipole-image dipole interaction, however, is contradicted by the experiments in a number of ways. In Sec. IV E it was found that the influence of the molecular dipole with respect to the surface normal, which is essentially M, is negligibly small. Furthermore, the K^2 dependence of Eq. (18) is not found, as can be seen in Sec. IV D. Therefore, one may conclude that the dipole component parallel to the angular momentum does not play an important role. Moreover, it was shown in Sec. IV C that for the $Q(12,2)$ and $Q(12,3)$ lines the effect disappears at low pressure although the excited-state dipole is 2.5% larger than the ground-state dipole.[22] Thus it can be concluded that the dipole is of little importance in explaining the dependence of α on J.

Another possible mechanism for the appearance of a pressure difference could be the flux of internal energy in the gas which accompanies the excitation of a certain velocity group. In excitation, the energy of the photon is transformed into internal energy of the molecule, both vibrational (positive and approximately equal for all transitions) and rotational (negative, almost zero, and positive for P, Q, and R lines, respectively). In the stationary state in a closed cell, the flux of internal energy will give rise to a temperature difference between the ends of the cell. This, in turn, can give rise to a pressure difference by the mechanism of thermal creep.[9] This mechanism seems to be ruled out by the following observations. First, the thermocouple signal monitoring the temperature gradient along the tube is found to be proportional to the laser power. This is probably due to incoupling losses of the laser light (and possibly to direct heating of the thermocouple by scattered light). Only at higher pressure, where the absorption in the gas becomes significant, the thermocouple also showed a signal proportional to the absorption in the gas. An odd-in-detuning signal, as expected from the internal heat flux and as required to account for the observed δp, was never seen. Second, the measured δp signals were not sensitive to whether or not the tube was temperature controlled. Third, the experiments indicate that the change in rotational state of the molecule is much more important for SLID than the change in the vibrational state; however, the change in vibrational energy is more than two orders of magnitude larger than the change in rotational energy for the $R(4,3)$ line. The fourth—and strongest—argument is that the sign of the experimentally measured pressure signals for the $R(4,3)$ is opposite to that expected from a thermal creep contribution associated with internal energy flux.

From the additional experiments described in Sec. IV D and IV E, it follows that orientation effects do not play a significant role in the results observed for the $R(4,3)$ transition. The increase in α must therefore be attributed to the increase in rotational quantum number $J=4\rightarrow 5$.

In conclusion, we have demonstrated that surface light-induced drift can be used to study the dependence of the accommodation coefficient, α, for parallel momentum transfer to the surface upon the internal state of the molecule. For methyl fluoride, CH_3F, it is found that the vibrational state is only of little influence on α. The rotational state of the molecule is found to be more important: Changing the rotational quantum number from $J=4$ to $J=5$ (with $K=3$) increases the value of α by 1.9×10^{-3} for a quartz surface at 295 K. Furthermore, the experiments show that the value of K/J (or the angle between the rotational axis and the figure axis) is of little importance for the value of α. Similarly, α is found to be insensitive to the orientation of **J** with respect to the surface. These observations also rule out a major role of the dipole in this process. This leaves the magnitude of J as a prime factor in determining α. A discussion of the role of J in this and related phenomena will be given in the framework of the unified kinetic theory developed by Borman *et al.*,[23] in a forthcoming paper.[20]

Experiments on surface light-induced drift for different surfaces are in progress. Preliminary results indicate that the value of $\delta\alpha$ is approximately a factor of 2 smaller for surfaces like stainless steel and platinum, and roughly a factor of 2 larger for Teflon and LiF.

ACKNOWLEDGMENTS

The authors would like to express their gratitude to P.L. Chapovsky, A. M. Shalagin, S. N. Atutov, M. I. Stockmann, and G. Nienhuis for most useful discussions and R. J. C. Spreeuw and A. de Raad for assistance in the experiments. This work is part of the research program of the Foundation for Fundamental Research on Matter (FOM) and was made possible by financial support from the Netherlands Organization for Scientific Research (NWO).

[1]F. Kh. Gel'mukhanov and A. M. Shalagin, Pis'ma Zh. Eksp. Teor. Fiz. **29**, 773 (1979) [JETP Lett. **29**, 711 (1979)].

[2]H. G. C. Werij and J. P. Woerdman, Phys. Rep. **169**, 145 (1988), and references therein.

[3]R. W. M. Hoogeveen, G. J. van der Meer, L. J. F. Hermans, and P. L. Chapovsky, J. Chem. Phys. **90**, 6143 (1989).

[4]A. V. Ghiner, M. I. Stockmann, and M. A. Vaksman, Phys. Lett. **96A**, 79 (1983).

[5]R. W. M. Hoogeveen, R. J. C. Spreeuw, and L. J. F. Hermans, Phys. Rev. Lett. **59**, 447 (1987).

[6]V. N. Panifilov, V. P. Strunin, and P. L. Chapovsky, Zh. Eksp. Teor. Fiz. **85**, 881 (1983) [Sov. Phys.—JETP **58**, 510 (1983)].

[7]D. T. Hodges, J. R. Tucker, and T. S. Hartwick, Infrared Phys. **16**, 175 (1976).

[8]V. R. Mironenko and A. M. Shalagin, Izv. Akad. Nauk SSSR, Ser. Fiz. **45**, 995 (1981) [Bull. Acad. Sci. USSR, Phys. Ser. **45**, 87 (1981)].

[9]E. A. Kennard, *Kinetic Theory of Gases* (McGraw-Hill, New York, 1938).

[10]S. K. Lee, R. H. Schwendemann, R. L. Crownover, D. D. Skatrud, and F. C. DeLucia, J. Mol. Spectrosc. **123**, 145 (1987).

[11]S. K. Lee, R. H. Schwendemann, and G. Magerl, J. Mol. Spectrosc. **117**, 416 (1986).

[12]L. C. Bradley, K. L. Soohoo, and C. Freed, IEEE J. Quantum Electron. **QE - 22**, 234 (1986).

[13]A. S. Casparian and R. H. Cole, J. Chem. Phys. **60**, 1106 (1974).

[14]In this notation the values between brackets denote J, the angular momentum quantum number of the ground-state level, and K, its projection on the figure axis. Together with excitation of the ν_3 vibrational mode, the value of J changes by -1, 0, and $+1$ (P, Q, and R lines, respectively), while the value of K remains unchanged.

[15]The error thus introduced may seem of order $1-\alpha$. However, in determining n_e from Eq. (17), a similar approximation $\alpha_e=1$ was used throughout. The combined result is that the error in the experimental value in terms of $\delta\alpha$ is of order $(1-\alpha)^2$ only.

[16]R. W. M. Hoogeveen, G. J. van der Meer, L. J. F. Hermans, A. V. Ghiner, and I. Kuščer, Phys. Rev. A **39**, 5539 (1989).

[17]G. J. van der Meer, R. W. M. Hoogeveen, L. J. F. Hermans, and P. L. Chapovsky, Phys. Rev. A **39**, 5237 (1989).

[18]R. W. M. Hoogeveen and L. J. F. Hermans, Phys. Rev. Lett. **65**, 1563 (1990).

[19]A. E. Bakarev and A. K. Folin, Opt. Spektrosk. **62**, 475 (1987) [Opt. Spectros. (USSR) **62**, 284 (1987)].

[20]R. W. M. Hoogeveen, L. J. F. Hermans, V. D. Borman, and S. Yu. Krylov, following paper, Phys. Rev. A **42**, 6480 (1990).

[21]P. L. Chapovsky (unpublished).

[22]S. M. Freund, G. Duxbury, M. Römheld, J. T. Tiedje, and T. Oka, J. Mol. Spectrosc. **52**, 38 (1974).

[23]V. D. Borman, S. Yu. Krylov, and A. V. Prosyanov, Zh. Eksp. Teor. Fiz. **94**, 271 (1988) [Sov. Phys.—JETP **67**, 2110 (1988)].